

Thickness Dependence of the Solvent-Induced Glass Transition in Polymer Brushes

Alexander Laschitsch, Charles Bouchard, Jörg Habicht, Martin Schimmel, Jürgen Rühle, and Diethelm Johannsmann*

Max-Planck-Institute for Polymer Research, Ackermannweg 10, D-55128 Mainz, Germany

Received May 11, 1998; Revised Manuscript Received November 16, 1998

ABSTRACT: We have investigated the sorption behavior of polystyrene brushes with thicknesses of 10–200 nm in toluene vapor. The sorption curve displays a kink, which is attributed to the solvent-induced glass transition. The derivative of the sorption curve with respect to solvent activity (“osmotic capacity”) shows a glass step at a certain characteristic activity a_g . This is the analogue of the glass step observed in the heat capacity at T_g with differential scanning calorimetry. Both a_g and the height of the glass step decrease with decreasing film thickness. The glass step is most pronounced after annealing the films at elevated temperatures in a vacuum. Due to accumulation of solvent in the film, the step disappears after repeated swelling/drying cycles.

Introduction

Polymers confined to thin films frequently have a structure and dynamics different from those in bulk.^{1,2} There are a number of different sources for these anomalies such as geometrical constraints, enthalpic interactions with the substrate, and enrichment of chain ends or impurities at the interface. A shift of the glass temperature T_g in thin films has been reported by a number of researchers. Early indications of a decreased T_g in thin films were reported by Reiter, who found that polystyrene (PS) films dewet silicon wafers at temperatures, where one would expect them to be immobile.³ Keddie and Jones have ellipsometrically investigated the thermal expansion of spin-cast polystyrene films on silicon wafers as a function of temperature.⁴ They find a glass step which they use to derive the glass transition temperature T_g . A decrease of T_g of up to 25 °C is observed for thin films. Wallace et al., on the other hand, find an increase of T_g for the same system using X-ray reflectometry.⁵ Apparently, the exact conditions at the substrate surface have a large influence and therefore must be characterized with care. DeMaggio et al. have used positronium lifetime spectroscopy to probe the internal free volume in thin polystyrene films on silicon wafers.⁶ They also find a decrease of T_g . Additionally, the authors report on a decreased thermal expansivity above T_g for the same samples. Monte Carlo simulations on polymers close to a free surface⁷ and a solid wall⁸ show that the dynamics is faster than in the bulk at the free interface, whereas it is slowed down close to the substrate. For a polymer melt confined between two solid walls, a strongly anisotropic mobility was found.⁹

Adopting the view that the glass transition is correlated to the free volume inside the film, one would conclude that the chains in films with decreased T_g are arranged such that they fill space less well than they do in the bulk. The free volume inside a polymer sample is affected not only by temperature but also by the addition of low molecular weight additives.¹⁰ The effect of plasticizers on the polymer dynamics is fairly well

described by a decrease of the glass temperature T_g . This implies that at a given temperature the glass transition can also be driven by the addition solvent. By gradually mixing plasticizing molecules into a polymeric material, its internal free volume is increased until at a certain solvent volume fraction ϕ_g the glass temperature T_g is lowered to room temperature and the material becomes soft. Conversely, if solvent is withdrawn from a polymer solution, the polymer will rigidify at about the same solvent content ϕ_g . The solvent chemical potential corresponding to ϕ_g we call μ_g and the corresponding solvent activity a_g , where activity and chemical potential are related by $\mu = k_b T \ln(a)$. We use the activity rather than the chemical potential to display the data, because the activity $a = p/p_{\text{sat}}$ (p the vapor pressure and p_{sat} the saturation vapor pressure) is closer to intuition and to the experimental procedure.

There is an analogy between the temperature-driven glass transition and the solvent-driven glass transition. In the same way as entropy is frozen in when a polymer melt is cooled to below T_g , the solvent is trapped in the polymer matrix when it is dried to below a_g . Below the glass transition, the rigidity of the matrix opposes its collapse. Free sites remain inside the polymer, which attract solvent molecules and therefore induce an excess solvent content. Provided that drying occurs slow enough, this excess solvent uptake is not a kinetic phenomenon caused by slow solvent transport, but an intrinsic property of the glassy polymer. The sorption curve $\phi_S(a)$ of polymeric glass formers displays a characteristic kink at the glass transition activity a_g .^{11–13} To emphasize the analogy with differential scanning calorimetry (DSC), we differentiate the sorption curve with respect to solvent activity a . We call the derivative $c_\pi = d\phi_S/da$ “osmotic capacity”. It is the analogue of the heat capacity in DSC. In particular, it displays the glass step.

Microweighing a polymeric film in solvent vapor therefore is a way to probe the film's glass transition. We report on the solvent-induced glass transition of polystyrene brushes. The term “brush” in this context refers to a dense layer of linear polymer chains that have been covalently bound to the substrate at one end.^{14–16} The reason for employing brushes rather than spin-cast films is simply that brushes do not dewet the

* To whom correspondence should be sent. Phone 49-6131-379 163; Fax 49-6131-379 360; e-mail johannsmann@mpip-mainz.mpg.de.

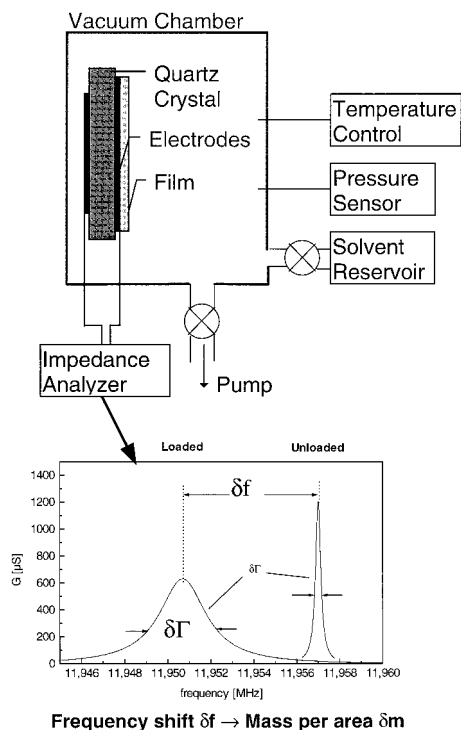


Figure 1. Schematic description of the experimental setup.

substrates, whereas spin-cast films frequently do. The brushes were grown on the surfaces of quartz resonators by the "grafting from" technique.^{17,18} The resonators are operated as quartz crystal microbalances.¹⁹ They are mounted inside a vacuum chamber. When toluene vapor is admitted to the chamber, the brushes swell. The mass of the brush/solvent system is monitored during slow drying ramps. The (de)sorption curves display the characteristic kink, which is analyzed as a function of drying speed, history, substrate properties, and—most importantly—brush thickness.

Theoretical Background

For polymer melts above the glass transition, sorption is usually described by the Flory–Huggins law²⁰

$$\mu_{\text{int}}^{\text{FH}}(\phi_p, T) = k_B T [\ln(1 - \phi_p) + \phi_p + \chi \phi_p^2] \quad (1)$$

where $\mu_{\text{int}}^{\text{FH}}$ is the solvent chemical potential, ϕ_p is the polymer volume fraction, and χ is the polymer–solvent interaction parameter. In diffusion equilibrium the solvent chemical potential in the film is equal to the chemical potential in the vapor phase given by

$$\mu_{\text{ext}} = k_B T \ln(a) = k_B T \ln(p/p_{\text{sat}}) \quad (2)$$

with a the activity, p the solvent vapor pressure, and p_{sat} the saturation vapor pressure. The Flory–Huggins law predicts a smooth dependence of solvent content on vapor pressure with a positive curvature everywhere. Close to a solvent volume fraction $\phi_s = 0$ the solvent content depends almost linearly on vapor pressure. This regime is sometimes called Henry sorption.

Below the glass transition one finds an excess solvent uptake and a negative curvature of the sorption line (Figure 2). It is sometimes explained as "Langmuir hole filling" or "dual mode sorption".¹² According to this view, the glassy polymer matrix does not collapse in the same

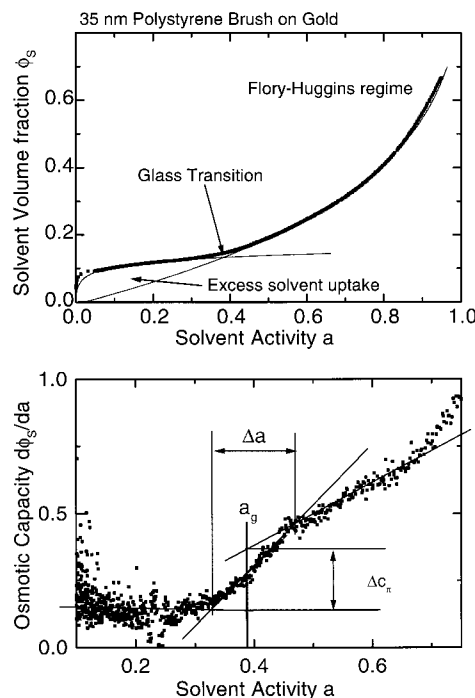


Figure 2. (a) Typical sorption curve. (b) Osmotic capacity, which is the derivative of the sorption curve from (a). The straight lines indicate the idealized glass transition.

way as a polymer melt. Some free sites remain which are populated by solvent molecules following Langmuir statistics. The dual mode picture suggests that the sorption has two separate components in parallel. The first one obeys the Flory–Huggins law and the second one the Langmuir isotherm. The sorption/desorption curve has a kink at the point where the solvent-induced plastification is just sufficient to lower T_g to ambient temperature.

Leibler and Sekimoto have put forward an alternative explanation for the excess solvent uptake which relies on internal stress rather than voids.¹¹ They assume that the polymer–solvent system is incompressible and that all loss of solvent is followed by matrix contraction. Below the glass transition, matrix contraction is opposed by its stiffness which is parametrized by an elastic modulus $K_{\text{gl}}(\phi_s)$. The resulting permanent internal stress enters the free energy as an elastic contribution. Assuming that $K_{\text{gl}}(\phi_s)$ is zero above the glass transition and a constant K_{gl}^0 below the glass transition, Leibler and Sekimoto write

$$\begin{aligned} \mu_{\text{int}}(\phi_p, T) &= \mu_{\text{int}}^{\text{FH}}(\phi_p, T) + \mu_{\text{int}}^{\text{LS}}(\phi_p, T) \\ &= k_B T [\ln(1 - \phi_p) + \phi_p + \chi \phi_p^2] - \nu_1 K_{\text{gl}}^0 \ln\left(\frac{\phi_p}{\phi_{p,g}}\right) \end{aligned} \quad (3)$$

where ν_1 is the solvent molecular volume and $\phi_{p,g}$ is the polymer volume fraction at the glass transition. Since the matrix collapse is achieved by local rearrangements of chains, the numerical value of K_{gl}^0 should be of the same order of magnitude as the macroscopic shear modulus, which is indeed the case. Equation 3 reproduces the excess solvent uptake near the glass transition quite well. While this equation is a convenient function for fitting, the interpretation of it is somewhat unclear. Presumably, both internal stress and voids contribute to the excess solvent uptake. It is not certain that the

fit parameter K_{gl}^0 can be straightforwardly interpreted as a local elastic modulus.

A caveat to be mentioned is the fact that the χ parameter often depends on concentration in the range of high polymer concentration.^{21–23} Flory dealt with this issue in his well-known equation-of-state approach.²⁴ However, these considerations entirely rest on equilibrium thermodynamics, while the glass transition is induced by a loss of ergodicity. A jump in the χ parameter right at the glass transition would be highly fortuitous. The kink in the sorption curve is observed for many different polymer–solvent systems and therefore cannot be assigned to an anomaly in the χ parameter.

In view of conceptual difficulties connected to a microscopic explanation of the kink in the sorption curve, we seek a description that avoids specific assumptions about the origin of the excess sorption as much as possible. We do not want to make a statement with regard to the microscopic origin of the excess solvent content, but rather use the excess solvent to probe the glass transition as a function of external parameters such as film thickness and drying speed. We take the view that the solvent chemical potential μ can be regarded as an intrinsic variable of state, which drives the glass transition in essentially the same way as temperature. On microscopic grounds, this point of view certainly is a simplification. Rössler et al. have probed the dynamics of the PS/toluene system with NMR.²⁵ Taking the dephasing time T_2 as a criterion for the glass transition, they can identify two separate glass transitions for the PS/toluene system, which they attribute to the two components. We believe that the glass transition observed in the sorption curve should be ascribed to the polystyrene component.

A conceptual difference between the solvent-driven and the temperature-driven glass transition is the possibility of annealing the sample in a vacuum at high temperatures. In this way, virtually all solvent is removed. There is no way of withdrawing all entropy in the temperature-driven glass transition, which would be the equivalent process to “annealing”. Interestingly, high-temperature annealing has a very profound effect on the sorption behavior of polymer brushes.

Treating the solvent chemical potential μ as an intrinsic variable of state, the solvent-induced glass transition is of pseudo-second-order in the Ehrenfest sense. The second derivative of the grand canonical potential Ξ with respect to solvent chemical potential μ has a step at the glass transition. For the grand canonical potential Ξ we write

$$\Xi = \Xi_0 + \mu N_S \quad (4)$$

where Ξ_0 contains all contributions independent of solvent content, and N_S is the number of solvent molecules inside the film. The number of solvent molecules N_S is related to the solvent volume fraction ϕ_S by

$$\phi_S = \frac{N_S V_S}{N_S V_S + N_P V_P} \quad (5)$$

where V_S and V_P are the molar volumes of solvent and polymer, and N_P is the number of polymer segments. We have assumed that the volume of mixing is zero. With eqs 4 and 5 the derivative $d\phi_S/da$ becomes

$$c_\pi = \frac{d\phi_S}{da} = \frac{d\phi_S}{dN_S} \frac{dN_S}{d\mu} \frac{d\mu}{da} = \left(\frac{d\phi_S}{dN_S} \frac{d\mu}{da} \right) \frac{d^2\Xi}{d\mu^2} \quad (6)$$

We call the derivative $d\phi_S/da$ “osmotic capacity” c_π . Some authors use the osmotic modulus $K_\pi = \phi_S dp/d\phi_S$ for a thermodynamic description rather than $d\phi_S/da$. We prefer to use the capacity in order to emphasize the analogy to differential scanning calorimetry. Apart from the prefactor in brackets, the osmotic capacity is the second derivative of the grand canonical potential with respect to solvent chemical potential. It corresponds to the heat capacity which is a second derivative of the free energy with respect to temperature. Because the prefactor is a smooth function of the activity a , the step in the second derivative $d^2\Xi/d\mu^2$ translates into a similar step in the osmotic capacity c_π . From the step in the osmotic capacity the glass transition activity a_g can be derived in the same way as T_g is determined from the specific heat in calorimetry.

Materials

The synthesis of the polymer brush followed the “grafting from” approach, which is described in detail in refs 17 and 18. The first step is the formation of a self-assembled monolayer of an initiator for free radical polymerization at the substrate surface. As substrates we mainly used bare gold. To investigate the influence of the substrate, we also performed experiments on SiO_x layers evaporated onto the gold electrode. The SiO_x surface is rougher than the gold surface and is known to have a porous structure. Also, SiO_x has an oxidic surface, which may affect the physical contacts between polymer chains and the substrate. Generally speaking, the results obtained on gold and SiO_x surfaces are similar. However, the data quality and reproducibility were better on gold substrates, which we attribute to the somewhat fragile structure of the SiO_x layer. Thermally evaporated SiO_x layers contain voids which may condense with time. Within the accuracy of our data, we see no differences between the different substrates.

The linker chemistry is based on thiols for gold surfaces and on monochlorosilyl moieties for SiO_x surfaces.²⁶ The initiators are derivatives of AIBN. After preparation of the self-assembled monolayer of initiator the polymerization is started in a solution of styrene monomer in toluene. The brush thickness is adjusted via polymerization time and monomer concentration. After polymerization, the samples are rinsed with solvent and undergo Soxhlet extraction with toluene for 15 h to remove physisorbed polymer. The molecular weight of a given sample is a priori unknown. A lower limit can be derived from reference experiments where the grafted material was cleaved off and investigated with size exclusion chromatography. From these investigations we conclude that the molecular weight is above $M_w \sim 100\,000$ g/mol with a polydispersity in the range of $M_w/M_n \sim 1.5$.

Polymer brushes are quite peculiar systems, whose behavior differs in a number of ways from bulk polymers.^{14–16} However, these anomalies are of minor interest in this context. Most of the special features of brushes are observed when the brushes are swollen in solvent or bulk polymer. Most importantly, chain stretching is observed in this case, which profoundly affects the physical properties of the substrate–brush–bulk system. Here, we work with collapsed brushes. While

chain stretching is still present for the thicker brushes, it is not expected to affect the glass transition because the physical processes underlying the glass transition are believed to occur on a local scale. This is, for example, evidenced by the fact that T_g is largely independent of molecular weight. By the same argument, the segmental dynamics and the friction coefficient should not be affected by whether the chain is attached at the bottom. Stretching should also be unimportant as long as the blob size²⁷ is larger than the dynamic correlation length, which is of the order of a few nanometers.²⁸ It seems noteworthy that solid-state NMR has given evidence for local nematic order even for bulk entangled polymers.²⁹ This kind of order should much outweigh the effects induced by the brush topology. Prucker et al. have carried out a systematic comparison of spin-cast films and brushes with respect to their thermal glass transitions and did not find a significant difference.³⁰

The residual chain stretching should not affect the equilibrium solvent content either. This contrasts with the situation found for brushes swollen in a good solvent. Here, chain stretching actually governs swelling, and the solvent content is a function of the distance z from the substrate. However, liquid-phase experiments on similar brushes have yielded a swelling ratio of at least 5. Only at this degree of swelling does chain stretching enter the free energy at a magnitude comparable to the solvent osmotic pressure. At the degree of swelling encountered here (15% at the glass transition), the solvent content is entirely governed by the χ parameter and the rigidity of the matrix. We therefore believe that the terminal attachment has a minor influence on the glass transition. The prime advantage of covalent attachment is the fact that it prevents dewetting. Dewetting proved to be a serious problem for sorption experiments on spin-cast films.

The thickness of the brushes was independently measured at different spots with ellipsometry.³¹ There was a slight lateral variation of thickness over the quartz plate of up to 15% of the average thickness. This is the horizontal error bar in Figure 6.

Experimental and Data Analysis

Details of the experimental setup have been described previously.³² A schematic description is given in Figure 1. All samples were annealed in a vacuum oven at 110 °C for 12 h prior to experiment. The AT-cut quartz blanks were mounted with alligator clamps. The temperature was kept constant at $T = 25.8 \pm 0.3$ °C during the whole experiment.

The resonator frequency was determined by impedance analysis.³³ We derived the resonance frequency by fitting a Lorentzian to the spectrum of the real conductance (Figure 1). The bandwidth of the resonance is automatically obtained as well. In some investigations we used a reference quartz in parallel to monitor pressure- or temperature-induced frequency drifts. Temperature–frequency coupling was completely negligible. We did observe a slight dependence of frequency on hydrostatic pressure as reported in the literature.³⁴ The magnitude of the effect never exceeded 1% of the film mass and has been neglected. There were no significant differences between the values of the solvent content determined from the different harmonics. We mostly used the fourth harmonic at 28 MHz.

For soft layers, one can in principle deduce viscoelastic information on the layers from the bandwidth and a

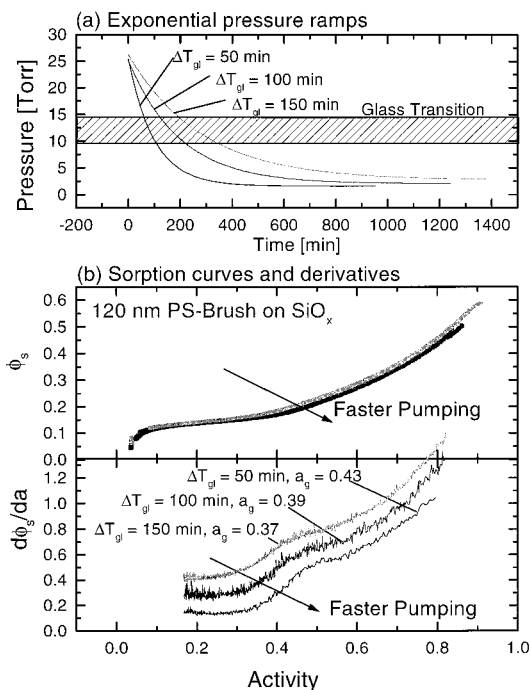


Figure 3. (a) Solvent vapor pressure vs time for three different drying speeds. (b) Sorption curves and osmotic capacity for a 120 nm polystyrene brush on SiO_x at different drying speeds. The glass transition activity a_g increases with increasing drying speed.

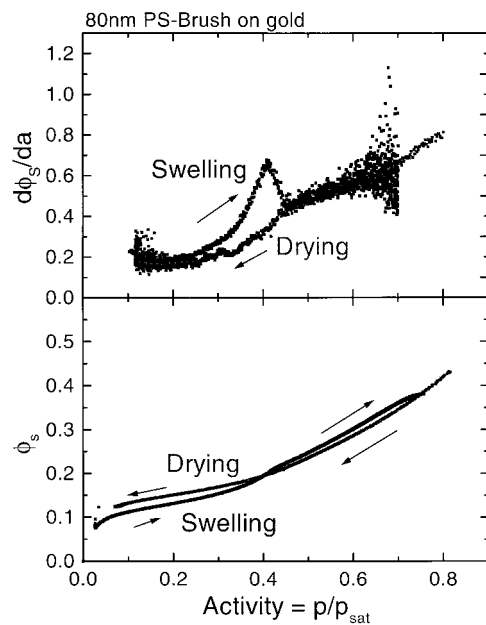


Figure 4. Comparison of swelling and drying kinetics. The swelling kinetics shows a strong overshoot shortly above the glass transition, which prevents a data analysis as sketched in Figure 2.

comparison of the frequency shifts on different harmonics.^{33,35} We indeed observe a substantial increase in bandwidth for highly swollen films. This softening is caused by the glass transition. However, viscous damping is connected to the megahertz glass transition which occurs at a much higher solvent concentration than the dc glass transition. Alig and co-workers have obtained similar information with a technique based on ultrasonic reflectometry.³⁶ The solvent-driven glass transition shifts with the frequency of the experiment in the same way as the temperature-driven transition. Therefore, we

do not discuss the bandwidth in the following and confine ourselves to the shifts in frequency, i.e., the film mass. The kink in the sorption curve is caused by the dc glass transition.

For highly swollen films, softening introduces an elastic correction to the apparent mass as determined by application of the Sauerbrey equation. There is a scheme to measure this effect and correct for it relying on the comparison of the frequency shifts on different overtones.³⁷ We only found small elastic effects for highly swollen brushes and neglect them in the following.

Another potential source of artifacts are stresses due to a lateral expansion of the polymer film. Elastic energy stored in the quartz may shift its resonance frequency due to small nonlinearities. Heusler et al. have measured the frequency shift induced by a difference in hydrostatic pressure between the two sides.³⁸ They find a parabolic dependence with a shift $\delta f \sim 100$ Hz for a pressure difference of about 10 kbar. An order of magnitude estimation using the yield stress of polystyrene and the equations of elastic beams shows that this effect is negligible here.

After mounting the samples, the chamber was first evacuated to about 10^{-2} Torr. Subsequently, toluene vapor was admitted. The pressure was adjusted to about 26 Torr, which corresponds to an activity of about 0.85. The saturation vapor pressure of toluene at 26 °C is 31 Torr.³⁹ We used MKS Baratron type 128 pressure sensors which work on a capacitive principle and therefore are suitable for many kinds of gases. The estimated error of the activity is about 0.01. After a steady state of film mass had been reached, the solvent vapor was withdrawn through a needle valve. The resulting pressure ramp has the shape of a single-exponential decay (Figure 3a). A typical time constant was 3 h. This pumping speed was chosen slow enough to ensure good diffusion equilibrium throughout the entire experiment.

We worked with decreasing rather than increasing pressure ramps for two reasons. First, the condition that the pumping rate has to be less than the diffusion time scale is more easily fulfilled with decreasing ramps. Initially, when pumping is fast, the diffusion is fast. Diffusion slows down as the film dries. At the same time the decrease of vapor pressure slows down as well. Second, it turned out that the glass steps were more easily observed on drying than on swelling. This is exemplified by the data set comparing swelling and drying shown in Figure 4. Upon swelling, there is an overshoot in the osmotic capacity $d\phi_S/da$. Presumably, this is connected to a fundamental difference between drying and swelling. During swelling large concentration gradients can build up inside the film because diffusion is faster for the parts already swollen than for the parts still dry. The swelling kinetics can be rather complex.⁴⁰ For drying, the phenomenology is simpler, because there is no solvent reservoir. The scheme of analysis used here can only be applied to data taken during drying.

The plasticizing effect of solvent is frequently described by writing

$$T_g = T_{g2} - k\omega_S \quad (7)$$

with T_{g2} the glass temperature of the pure polymer, ω_S the solvent weight fraction, and k a constant. For the PS/toluene system the constant k is about 500°. ^{41,42} In

accordance with the literature, T_g is lowered to room temperature at a solvent volume fraction of about $\omega_S = 0.14$.

The frequency shifts were converted to a mass per unit area δm with the Sauerbrey equation¹⁹

$$\delta m = -\frac{Z_q}{2f_0} \frac{\delta f}{f} \quad (8)$$

with $Z_q = 8.8 \times 10^6$ kg m⁻² s⁻¹ the impedance of AT-cut quartz, f_0 the fundamental frequency, δf the frequency shift, and f the frequency of the harmonic used for measurement. It is known that the Sauerbrey equation is in practice only accurate within some percent.³⁵ This error cancels when the solvent mass is normalized to the film mass to obtain the solvent mass fraction ω_S . The solvent volume fraction ϕ_S was derived according to eq 5.

The osmotic capacity was analyzed in the same way as it is usually done for DSC data. Figure 2 shows a typical data set and illustrates how the parameters are derived. We manually set limits between three regions and fit straight lines to the data sets in the different regions. These straight lines represent the idealized glass step. The center of the step is the glass activity a_g , and the width of the transition is Δa . The magnitude of the step Δc_π is determined by extrapolating the lines from below a_g and above a_g to a_g and reading their difference (Figure 2b). Finally, we obtain the solvent volume fraction at the glass transition $\phi_g(a_g)$ from the sorption curve $\phi_S(a)$.

Results and Discussion

Influence of Pumping Speed. Sorption experiments on glass formers in the bulk are very time-consuming because the diffusion equilibrium is approached only very slowly. However, the diffusion time scale $\tau_D = l^2/D$ scales with the square of the film thickness l . For a film thickness in the range of 100 nm, τ_D is on the order of a few minutes, and "quasi-stationary" drying experiments become feasible. The term "quasi-stationary" here implies that diffusion equilibrium is largely maintained. Diffusion equilibrium does not, however, imply thermodynamic equilibrium. There may be intrinsic mechanical relaxations on the time scale of weeks and months even for very thin films. These relaxations are not governed by the solvent transport dynamics, but rather by a reorganization of the local structure.

The fact that the drying dynamics is governed by intrinsic dynamics rather than transport dynamics is evidenced by an increase of the glass transition chemical potential μ_g with increasing drying speed. Figure 3b shows sorption data obtained on a 120 nm brush taken at different pumping speeds. The evolution of pressure with time closely follows a single exponential with the time constants $\tau = 100, 200$, and 300 min. The effect of drying speed is most critical when the film crosses the glass transition, which happens at about $p = 12$ Torr. In the range between 15 and 10 Torr the pressure ramp is fairly linear. It takes $\Delta T_{gl} = 50, 100$, and 150 min to cross the range from 15 to 10 Torr for the three different pumping speeds. This time ΔT_{gl} has to be compared to the characteristic time for diffusion τ_D . We have determined this time in separate pressure step experiments to be less than 10 min for all samples. This result is in accordance with an estimate of τ_D from the diffusion

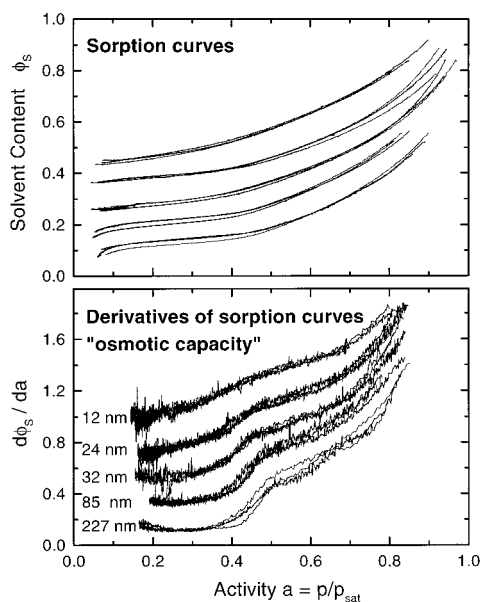


Figure 5. Sorption curves and osmotic capacities for polystyrene brushes on gold. Data sets for different thicknesses have been vertically displaced for clarity. All samples have been measured three times. They were annealed at high temperature between different runs.

constants given in ref 43. The comparison shows that the experimental time scale is longer than the diffusion time scale. Figure 3b shows the sorption curves and their derivatives. Clearly, the glass transition shifts to lower activities for slower pumping. This shift is not caused by a deviation from diffusion equilibrium. If this were the case, the solvent chemical potential in the vapor phase would be less than the chemical potential inside the film. In the case of insufficient equilibration during fast pumping the apparent glass activity would be *lowered*. The opposite is observed, proving that the shift of a_g with pumping speed is an intrinsic phenomenon.

A shift of T_g with cooling speed is well-known from calorimetric experiments. If the glass transition region

is crossed quickly, the material is trapped in a state less dense and less relaxed than for slow cooling. Our findings appear to correspond to this phenomenon. When the drying occurs quickly, the polymer matrix is trapped in a less dense state than the one found when drying is performed slowly. Because the solvent diffusivity strongly depends on the density of the matrix, fast drying should advantageously affect the removal of residual solvent in later stages of drying. Small amounts of volatile organic components in packaging materials are a very critical issue for environmental reasons. Traces of residual solvent are very hard to remove from glassy films. Following the above considerations, the glassy film may have a somewhat open architecture, if it was dried quickly enough. Rapid drying in early phases of the process will therefore be beneficial for the removal of residual solvent in the final state of drying.

Influence of Thickness. Figure 5 shows the sorption curves and the osmotic capacities obtained for brushes with different thicknesses on gold. The data have been vertically displaced for clarity. The osmotic capacity $c_\pi = d\phi_s/da$ displays the glass step more clearly than the sorption curves $\phi_s(a)$ themselves. The fact that the osmotic capacity above T_g is not a constant but increases with solvent content is caused by the functional form of the Flory–Huggins law. The sorption curve in the melt regime is curved upward, which results in an increase in osmotic capacity.

The derived fit parameters are given in Figure 6. The open squares are the fit parameters determined for each measurement. The error bars are derived from the fitting of the straight lines to the various sections of the data set (cf. Figure 2b). The full dots are the averages from the different measurements. The error bars on the full dots are either the averaged errors from the individual data points divided by $N^{1/2}$ (N is the number of measurements) or the standard deviation from the different measurements, whichever is larger.

The height of the glass step Δc_π decreases with decreasing thickness. Also, the glass step shifts to lower activities a_g and—with the exception of the 12 nm sample—to a lower solvent content ϕ_g . The 12 nm sample

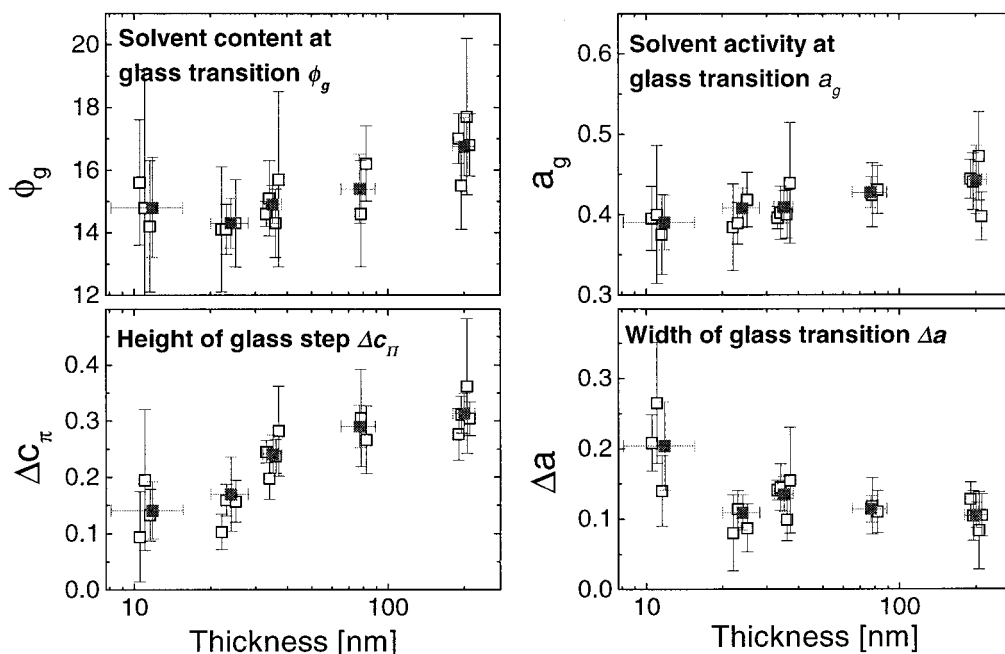


Figure 6. Derived parameters for polystyrene on gold.

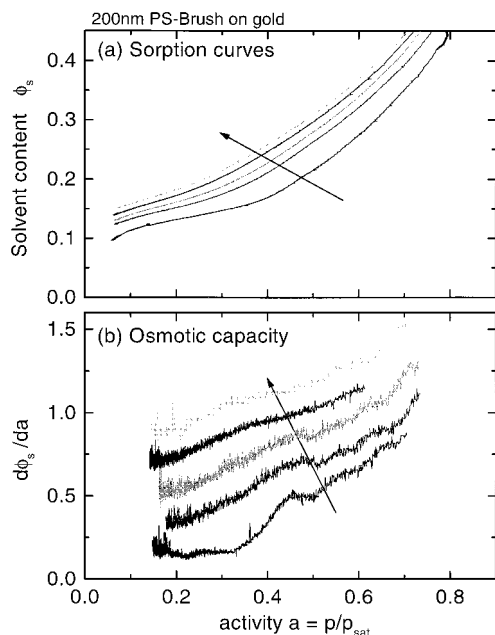


Figure 7. Repeated drying experiments on the 200 nm sample *without* high-temperature annealing between the different runs: (a) sorption curves and (b) derivatives (osmotic capacity). The arrows indicate the order in which the experiments were performed. In this case the sorption curves were *not* displaced vertically for clarity. There is an irreversible accumulation of solvent in the film. The glass transition gradually disappears.

appears to be somewhat exceptional because it has an increased ϕ_g and also a substantially larger width of the glass transition Δa .

Generally, our findings are in line with the previous observations on the temperature-driven glass transition.^{4,6} A connection between the solvent content at the glass transition ϕ_g and the glass transition temperature T_g is made by eq 7. For polystyrene the constant k is about 500°.^{41,42} With this value a decrease in ϕ_g of 2% translates into a decrease in T_g of about 10°. Therefore, the orders of magnitude of the observed effects roughly

agree. Thin films appear to contain more free volume than thick films. Presumably, they are packed less densely than the bulk material. The variation of the fit parameters with thickness appears to be rather continuous. From our data we cannot determine a characteristic thickness for the occurrence of thin-film anomalies.

Influence of History. Given that a true equilibrium is never reached in the glassy state, it is not surprising to find effects of history on drying as well. In Figure 7 we show sorption data on the 200 nm sample obtained with repeated wet/dry cycles, where no high-temperature annealing was done between different runs. In this case the sorption curves were *not* displaced vertically, for clarity. There is an irreversible accumulation of solvent in the film. The same effect could not be induced by just keeping the films in the wet state for long times. Evidently, the wet state reached after swelling freshly annealed brushes in solvent vapor for an extended time is not a true equilibrium state. Repeated cycling through the dry and the wet state causes an internal reorganization of the polymeric material which would take much longer without these swelling and drying steps. It seems doubtful whether the situation reached after repeated cycling is closer to a thermodynamic equilibrium than the freshly annealed state. If the dynamics of solvent uptake is more efficient than the dynamics of solvent removal, solvent will accumulate in the film for purely kinetic reasons. The fact that equilibrium is practically unachievable for surface bound polymers even in the presence of substantial amounts of solvent has been reported previously by Granick and co-workers.^{44,45} This group was interested in the properties of physisorbed polymers and concluded that the conditions of preparation were by far the most important factor determining the properties of the polymer layers. The dynamics of reorganization appeared to be exceedingly slow due to the attachment of the chains to the substrate. Presumably, the situation is similar here. Figure 8 shows the derived fit parameters for the repeated dry/wet cycles. Interestingly, the glass transition activity a_g depends

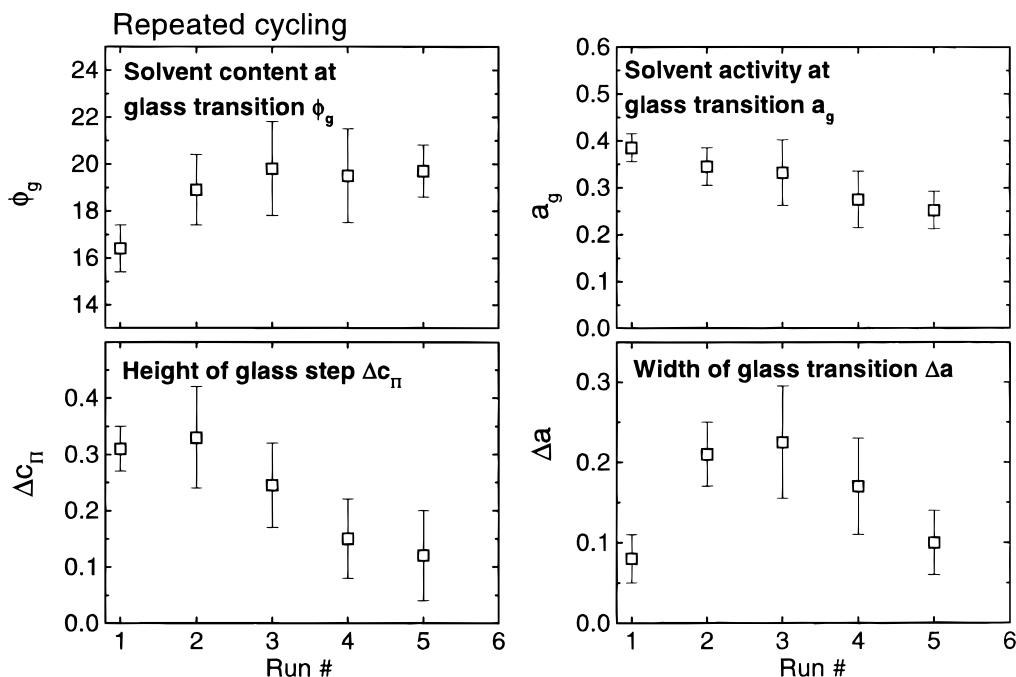


Figure 8. Fit parameters for repeating cycling through the dry and wet state for the 200 nm sample.

much more on history than the critical solvent volume fraction ϕ_g . There seems to be a certain amount of immobile solvent inside the film which affects the glass transition, although it does not take part in the solvent transport.

Acknowledgment. We acknowledge helpful discussions with Catherine Allain and Beatrice Guerrier as well as some help in the experiments by Anne-Claire Saby.

References and Notes

- (1) Sanchez, I. C., Ed. *Physics of Polymer Surfaces and Interfaces*; Butterworth: London, 1992.
- (2) Binder, K. *Adv. Polym. Sci.* **1994**, *112*, 258.
- (3) Reiter, G. *Europhys. Lett.* **1993**, *23*, 579.
- (4) Keddie, J. L.; Jones, R. A. L.; Cory, R. A. *Europhys. Lett.* **1994**, *27*, 59.
- (5) Wallace, W. E.; van Zanten, J. H.; Wu, W. L. *Phys. Rev. E* **1995**, *52*, R3329.
- (6) DeMaggio, G. B.; Frieze, W. E.; Gidley, D. W. *Phys. Rev. Lett.* **1997**, *78*, 1524.
- (7) Mansfield, K. F.; Theodorou, D. N. *Macromolecules* **1991**, *24*, 6283.
- (8) Baschnagel, J.; Binder, K. *Macromolecules* **1995**, *28*, 6808.
- (9) Baschnagel, J.; Binder, K. *J. Phys. I* **1996**, *6*, 1271.
- (10) Ferry, J. D. *Viscoelastic Properties of Polymers*; Wiley: New York, 1980.
- (11) Leibler, L.; Sekimoto, K. *Macromolecules* **1993**, *26*, 6937.
- (12) Berens, A. R. *Polym. Eng. Sci.* **1980**, *20*, 95.
- (13) Vrentas, J. S.; Vrentas, C. M. *Macromolecules* **1991**, *24*, 2404.
- (14) Halperin, A.; Tirell, M.; Lodge, T. P. *Adv. Polym. Sci.* **1991**, *100*, 31.
- (15) Szleifer, I.; Carignano, M. A. *Adv. Chem. Phys.* **1996**, *XCIV*, 165.
- (16) Grest, G. S.; Murat, M. In *Monte Carlo and Molecular Dynamics Simulations in Polymer Science*; Binder, K., Ed.; Clarendon Press: Oxford, 1994.
- (17) Prucker, O.; R  he, J. *Macromolecules* **1998**, *31*, 592.
- (18) Prucker, O.; R  he, J. *Macromolecules* **1998**, *31*, 602.
- (19) Sauerbrey, G. *Arch. Elektrotech.   bertragung* **1964**, *18*, 617.
- (20) Flory, P. J. *Principles of Polymer Chemistry*; Cornell University Press: New York, 1953.
- (21) Brandrup, J.; Immergut, E. H. *Polymer Handbook*, 3rd ed.; Wiley: New York, 1989.
- (22) Noda, I.; Higo, Y.; Ueno, N.; Fujimoto, T. *Macromolecules* **1984**, *17*, 1055.
- (23) Brostow, W. *Macromolecules* **1971**, *4*, 742.
- (24) Flory, P. J. *J. Am. Chem. Soc.* **1965**, *87*, 1833.
- (25) R  ssler, E.; Sillescu, H.; Spiess, H. W. *Polymer* **1985**, *26*, 203.
- (26) Habicht, J. Ph.D. Thesis, Universit  t Mainz, 1998.
- (27) de Gennes, P. G. *J. Phys. (Paris)* **1976**, *37*, 1443.
- (28) Schick, C.; Donth, E. *Phys. Scr.* **1991**, *43*, 423.
- (29) Graf, R.; Heuer, A.; Spiess, H. W. *Phys. Rev. Lett.* **1998**, *80*, 5738.
- (30) Prucker, O.; Christian, S.; Bock, H.; R  he, J.; Frank, C. W.; Knoll, W. *Makromol. Chem. Phys.* **1998**, *199*, 1435.
- (31) Azzam, R. M. A.; Bashara, N. M. *Ellipsometry and Polarized Light*; Elsevier: Amsterdam, 1987.
- (32) Bouchard, C.; Guerrier, B.; Allain, C.; Laschitsch, A.; Saby, A.-C.; Johannsmann, D. *Appl. Polym. Sci.* **1998**, *69*, 2235.
- (33) Domack, A.; Johannsmann, D. *J. Appl. Phys.* **1996**, *80*, 2599.
- (34) Stockbridge, C. D. *Vacuum Microbalance Techniques*; Plenum: New York, 1966; Vol. 5.
- (35) Wolff, O.; Seydel, E.; Johannsmann, D. *Faraday Discuss.* **1997**, *107*, 91.
- (36) Alig, I.; Lellinger, D.; Sulimma, J.; Tadjbakhsh, S. *Rev. Sci. Instrum.* **1997**, *68*, 1536.
- (37) Domack, A.; Johannsmann, D. *J. Appl. Phys.* **1996**, *80*, 2599.
- (38) Heusler, K. E.; Grzegorzewski, A.; J  ckel, L.; Pietrucha, J. *Ber. Bunsen-Ges. Phys. Chem.* **1988**, *92*, 1218.
- (39) Lide, D. R., Ed. *Handbook of Chemistry and Physics*, 76th ed.; CRC Press: Boca Raton, FL, 1995.
- (40) For a review see: Neogi, P. *Diffusion in Polymers*; Dekker: New York, 1996.
- (41) Ferry, J. D. In ref 40, p 488.
- (42) Chow, T. S. *Macromolecules* **1980**, *13*, 362.
- (43) Gall, T. P.; Kramer, E. J. *Polymer* **1991**, *32*, 265.
- (44) Hu, H.-W.; Granick, S. *Science* **1992**, *258*, 1339.
- (45) Hu, H.-W.; Granick, S.; Schweizer, K. S. *J. Non-Cryst. Solids* **1994**, *172–174*, 721.

MA980743T